

## Attractor geometry of a quasiperiodically perturbed, two-level atom

J. C. Camparo and R. P. Frueholz

Chemistry and Physics Laboratory, The Aerospace Corporation, P.O. Box 92957, Los Angeles, California 90009

(Received 2 July 1990)

We consider the behavior of a two-level atom interacting with a quasiperiodic, resonant field from the perspective of dynamical systems theory. In particular, we analyze the geometry of the phase-space attractor for the atomic system and find that there are basically only two types of attractor geometry, even though the atom's temporal evolution is very complicated. The dynamics giving rise to these two geometries are differentiated by the degree of adiabaticity associated with the field's variations, and in the regime of adiabatic dynamics, the attractor shows evidence of a noninteger scaling dimension. This result was unexpected, since *linear* dynamical systems are not known to give rise to strange attractors. We attribute the attractor's fractal nature to the scaling behavior of Bloch vector trajectories in the rotating reference frame.

### I. INTRODUCTION

The response of matter to rapid, deterministic electromagnetic-field fluctuations is an area of considerable present interest, spanning many different disciplines. In optical and nuclear physics it has been found that rapid phase switching can produce short, intense pulses of optical and  $\gamma$ -ray photons.<sup>1,2</sup> In chemical physics studies of amplitude and phase-tailored radiation pulses have lead to improvements in both NMR and optical spectroscopy (e.g., spectroscopic resolution),<sup>3</sup> and in atomic physics phase-controlled fields have been used to selectively excite dressed-atom states.<sup>4</sup> Yet despite these activities, little can really be said concerning the *general* dynamical behavior of quantum systems in the presence of rapidly fluctuating fields. This situation is not difficult to understand. As soon as the pattern of fluctuations becomes at all detailed, the dynamical complexity of even the simplest quantum system becomes excessive.<sup>5</sup> Consequently, it becomes difficult to categorize, let alone quantify, the quantum system's temporal evolution as a function of various physical parameters like field-matter interaction strength, quantum system relaxation rate, or phase-variation rate.

Consider the internal dynamics that arise when a simple two-level atom is perturbed by a quasiperiodic field. Recently, this problem has attracted a fair amount of attention,<sup>6-12</sup> since it was found that the *linear* density-matrix equations describing the interaction can yield nearly  $\delta$ -correlated dynamics, reminiscent of the chaotic dynamics observed in nonlinear systems. Figure 1(a) shows the temporal evolution of a two-level atom interacting with a field whose phase variation is the simple superposition of a sinusoid and square wave. (This particular field-atom interaction will be discussed more fully in Sec. II.) The figure was generated by numerically solving the optical Bloch equations for the quasiperiodic field,<sup>13</sup> and Fig. 1(b) shows the result of a discrete Fourier transform of the population difference between the two states. As can be seen, the temporal behavior of the pop-

ulation difference is quite complex, and its Fourier transform is broadband, even though the field's phase variations are relatively uncomplicated. Consequently, with the information contained in Figs. 1(a) and 1(b), it is difficult to correlate the atomic system's dynamics with, for example, field-atom interaction strength.

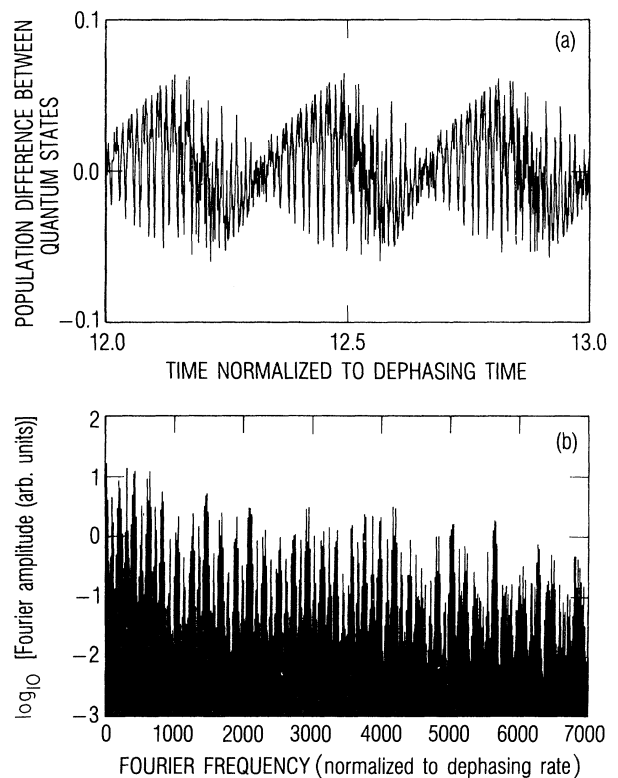


FIG. 1. (a) Temporal evolution of a two-level atom's population difference for a quasiperiodic resonant electromagnetic field:  $\Omega = 1200$ ,  $T_{sq} = 0.02$ ,  $\omega_s = 8\pi\sqrt{2}/T_{sq}$ . (b) Fourier spectrum of the dynamics illustrated in (a).

A similar, if not more troublesome, situation exists in the area of nonlinear dynamics and chaos that was alluded to above. Here too the dynamics can become exceedingly complex, exhibiting many characteristics often associated with stochastic processes. Yet in recent years significant progress has been made in devising analytical tools and measures for both computation and experimentation that can categorize and quantify the dynamics.<sup>14</sup> In the present work we employ some of these measures; in particular, the Grassberger-Procaccia correlation dimension,<sup>15</sup> to study the dynamical behavior of a two-level atom interacting with a field whose phase fluctuations are quasiperiodic.

Our purpose in this study is twofold. Primarily, our goal is to use these measures to quantify the atom's dynamical behavior, so that the atom's response to a quasiperiodic field can be studied as a function of the field-atom interaction strength. As will be shown below, even though the temporal behavior of the atom is quite complex, the atom's response essentially falls into one of only two categories. The parameter differentiating these categories is the degree of adiabaticity associated with the field's fluctuations. Our secondary intent is to demonstrate the general usefulness of these measures for investigating complicated, yet nonchaotic atomic dynamics. Specifically, these measures offer a convenient means of studying the complicated dynamics that arise when a quantum system interacts with a fluctuating electromagnetic field.

## II. SYSTEM OF EQUATIONS DESCRIBING THE FIELD-ATOM INTERACTION

In the present work we are concerned with the atomic dynamics that are induced by a classical electromagnetic field, when the phase  $\theta(t)$  of the field varies in a quasiperiodic fashion. To describe the atom's response to the field we employ the optical Bloch equations (i.e., two-level density-matrix equations), and include phenomenological relaxation rates  $\gamma_1$  and  $\gamma_2$ .<sup>13</sup> These equations are derived from the Schrödinger equation, and describe the response of an ensemble of two-level atoms to a classical electromagnetic field in a nonperturbative fashion. The atomic ensemble's response to the field depends on the fractional population in one of the atomic states; for example, the lower atomic state ( $\sigma_{11}$ ); and the degree of atomic coherence ( $\sigma_{21}$ ), where coherence refers to the superposition of ground and excited atomic-state wave functions. The two phenomenological rates  $\gamma_1$  and  $\gamma_2$  describe population relaxation of the two-level atom and atomic coherence dephasing, respectively. It is important to note that previous studies of this problem have not included relaxation in the dynamics,<sup>6-12</sup> consequently, attractors for the atomic dynamics could not exist.<sup>14</sup>

With regard to the field's phase and its temporal variations we let

$$\theta(t) = \theta_1(t) + \theta_2(t), \quad (1)$$

where

$$\theta_1(t) = \pi \sin(\omega_s t) \quad (2a)$$

and

$$\theta_2(t) = \pi H(t). \quad (2b)$$

Here,  $H(t)$  represents a square wave varying between 0 and 1 with a period of  $T_{sq}$ . Though this is only one of the many possible quasiperiodic functions that could be associated with  $\theta(t)$ , our particular choice was not arbitrary: it evolved out of our interest in atomic interactions with phase fluctuating fields,<sup>16</sup> a desire to make contact with previous investigations on kicked quantum systems,<sup>7,9,10</sup> and a desire to model an experimentally realizable situation.<sup>16,17</sup>

The complete system of equations for the atom's response to the field in autonomous form<sup>14</sup> is

$$\dot{X} = -\gamma_2 X - \Delta Y + \Omega Z \sin(\theta_1 + \theta_2), \quad (3a)$$

$$\dot{Y} = \Delta X - \gamma_2 Y + \Omega Z \cos(\theta_1 + \theta_2), \quad (3b)$$

$$\begin{aligned} \dot{Z} = & -\Omega X \sin(\theta_1 + \theta_2) - \Omega Y \cos(\theta_1 + \theta_2) \\ & + \gamma_1 (Z_0 - Z), \end{aligned} \quad (3c)$$

$$\dot{\theta}_1 = \omega_s (\pi^2 - \theta_1^2)^{1/2}, \quad (3d)$$

and

$$\begin{aligned} \dot{\theta}_2 = & \pi \sum_k (-1)^k \delta(f(\theta_1) - kT_{sq}/2), \\ f(\theta_1) = & \omega_s^{-1} \arcsin(\theta_1/\pi) = t. \end{aligned} \quad (3e)$$

Here  $\Omega$  is the Rabi frequency, which describes the strength of the field-atom interaction,  $\Delta$  is the detuning of the field from resonance, and the triplet  $(X, Y, Z)$  indicates the coordinates of the Bloch vector in the rotating frame. As a result of relaxation the norm of the Bloch vector is not a constant, but can vary between 0 and 1, and in the absence of a field the equilibrium value of the Bloch vector has  $X = Y = 0$  and  $Z = Z_0$ . The Bloch-vector coordinates are related to the elements of the two-level density matrix in a straightforward way:  $X = 2 \operatorname{Re}(\sigma_{21})$ ,  $Y = 2 \operatorname{Im}(\sigma_{21})$ , and  $Z = 1 - 2\sigma_{11}$ . Though it would appear that the autonomous form of these equations comprise a nonlinear system with five degrees of freedom  $(X, Y, Z, \theta_1, \theta_2)$ , when the equations are written nonautonomously it becomes clear that the system is in fact linear.<sup>18</sup> The advantage in considering the autonomous system of equations is that the phase-space coordinates for the system's attractor are immediately apparent, and it is our purpose to quantify the atom's complicated dynamics by the attractor's geometry.

For the problem under consideration the attractor exists in a five-dimensional space, whose coordinate axes can be labeled by  $X, Y, Z, \theta_1$ , and  $\theta_2$ . Considering just the phase components of the field, we note that, in general,  $\theta_1$  and  $\theta_2$  form a 2-torus when  $\dot{\theta}_1$  and  $\dot{\theta}_2$  are continuous and incommensurate. However, these quantities do not form a 2-torus in the present problem, since  $\theta_2$  can take on just two discrete values ( $\pi, -\pi$ ). It is reasonable therefore to associate the attractor geometry with a lower four-dimensional (4D) space, whose coordinate axes are taken as  $X, Y, Z$ , and  $\theta$ . With regard to the attractor characteristics to be discussed below, there was no

difference in the results on comparing attractor analyses in the 4D space with those obtained in the 5D space.

Normalizing the time scale to the intrinsic relaxation time  $1/\gamma$  ( $\gamma_1=\gamma_2=\gamma$ ), and letting  $Z_0=-1$  and  $\Delta=0$ , we consider the specific case of incommensurate sinusoidal and square-wave frequencies:  $T_{\text{sq}}=0.02$  and  $\omega_s=8\pi\sqrt{2}/T_{\text{sq}}$ . Additionally, since  $\omega_s$  is the fastest rate associated with the perturbation's variations, we define a quantity  $\eta$  equal to  $\Omega/\omega_s$ . We will refer to this quantity as an "adiabaticity parameter," since it is essentially a measure of how adiabatically the perturbation varies.<sup>19</sup> If  $\eta$  is much less than unity, then the atom cannot keep track of the various values of the field's phase, so that the fluctuations are nonadiabatic. Alternatively, if  $\eta$  is much greater than unity, then the atom easily follows all the field's variations, so that the fluctuations are adiabatic. Our choices for the magnitudes of  $T_{\text{sq}}$  and  $\omega_s$  were in part dictated by a desire to have a nonadiabatic regime of dynamics that would nonetheless correspond to a "strong"-field situation (i.e.,  $\Omega \gg \gamma$ ).

The above equations of motion were solved using a fourth-order Runge-Kutta method with adaptive step size.<sup>20</sup> (Step size was controlled by requiring the error in the computation of any of the Bloch-vector components to be less than  $10^{-7}$ ; decreasing this limit to  $10^{-11}$  had no significant effect on the results.) To insure that initial transients had died away and that the system's dynamics had reached the attractor, the solution was propagated to  $t=12$  prior to accumulating data for study. For a particular choice of computational parameters we typically analyzed the numerical solution between  $t=12$  and 100; this was to insure that many attractor orbits were sampled.

### III. RESULTS

#### A. Poincaré sections

As a first step in understanding the atomic dynamics, one can consider double Poincaré sections<sup>14</sup> of the attractor. A double Poincaré section may be formed by plotting  $X, Y$  attractor coordinates for specific values of the pairs  $Z, \dot{Z}/|\dot{Z}|$  and  $\theta, \dot{\theta}/|\dot{\theta}|$ . The value of these double Poincaré sections is that they provide a kind of cross-sectional view of the attractor. However, we have found it more informative to consider whole families or groups of double-Poincaré sections. Each group is associated with a particular value of  $Z, \dot{Z}/|\dot{Z}|$ , and contains all double-Poincaré sections associated with this pair. When a single double-Poincaré section is considered, only a small portion of the accessible  $xy$  plane is actually viewed. When a group of double-Poincaré sections is considered, though, the entire accessible  $xy$  plane is made manifest. This full  $xy$  plane pattern is the object of most interest, since our primary concern is with the atomic dynamics and not the superimposed phase variations of the field. In essence, these double-Poincaré section groups are cross-sectional slices of the Bloch vector's trajectory in the rotating coordinate frame.

Three separate double-Poincaré section groups, or for the sake of brevity, Poincaré sections, are illustrated in Fig. 2 for three different values of the Rabi frequency.

The  $xy$  plane of these figures cuts the  $z$  axis at the average value of  $Z$  (which varies between  $-1$  and  $0$  as  $\Omega$  increases), and  $\dot{Z}/|\dot{Z}|=+1$ . Figure 2(a) corresponds to  $\Omega = 17772$ , the adiabatic regime of dynamics; Fig. 2(b) corre-

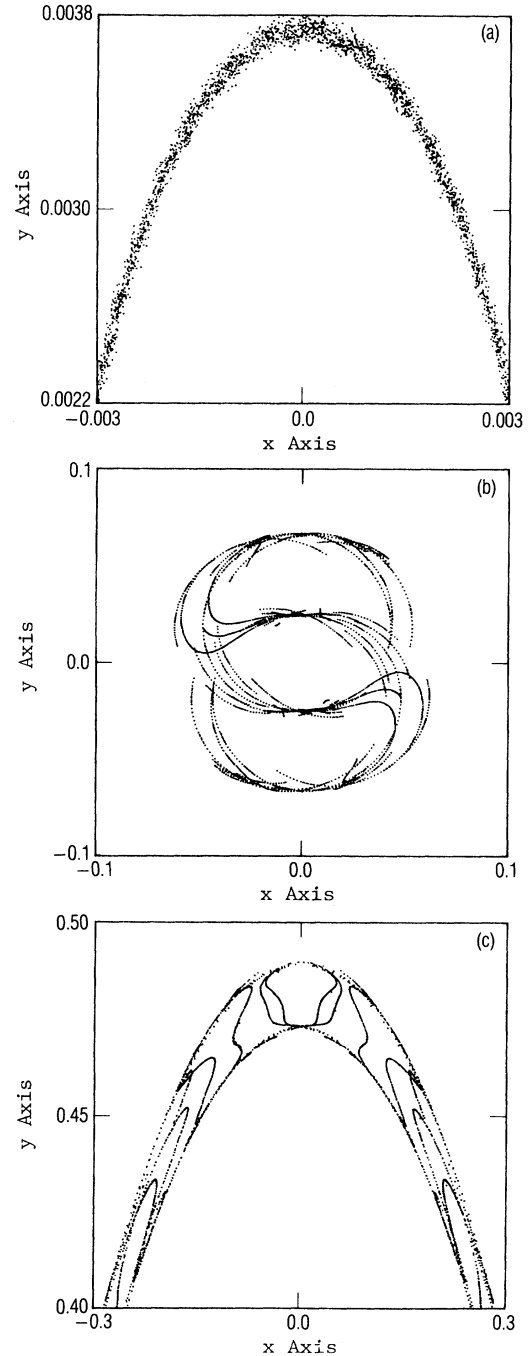


FIG. 2. Poincaré sections of the Bloch vector's motion through the rotating coordinate system's  $xy$  plane ( $dZ/dt > 0$ ). The  $xy$  plane cuts the  $z$  axis at the average value of  $Z$ , which varies between  $-1$  and  $0$  as  $\Omega$  increases. (a) Partial section of the adiabatic regime with  $\Omega = 17772$ . (b) Intermediate regime with  $\Omega = 1200$ . (c) Partial section of nonadiabatic regime with  $\Omega = 300$ .

sponds to  $\Omega = 1200$ , an intermediate regime of dynamics; and Fig. 2(c) corresponds to  $\Omega = 300$ , the nonadiabatic regime of dynamics. Similar appearing plots of the Poincaré sections were obtained for other values of  $\Omega$  in the three separate regimes of adiabaticity. In the adiabatic regime the Poincaré section yields an annulus, and when Poincaré sections at other values of  $Z$  (for this value of  $\Omega$ ) are examined it becomes clear that the Bloch-vector trajectory is a spheroidal shell. Furthermore, as evidenced by the seemingly uncorrelated points within the annulus, the volume of the shell is uniformly covered; this may indicate that the atomic system's trajectory visits different attractor regions with equal probability (i.e., the attractor is uniformly covered). In the intermediate regime of adiabaticity the Poincaré section is quite different. A highly structured and twisted Bloch-vector trajectory is found, and Poincaré sections similar to that shown in Fig. 2(b) are obtained both above and below the average  $Z$  value's  $xy$  plane. This twisting geometry persists into the nonadiabatic regime as shown in Fig. 2(c), except that the overall appearance of the Poincaré section is again annular. The coverage of the annulus, however, is no longer

uniform, indicating perhaps an attractor with regions that are visited by the atomic system's trajectory more often than others.

Investigating the nonadiabatic regime of the dynamics in more detail, we consider a Poincaré section that cuts the  $yz$  plane at  $X=0$  as well as Poincaré sections that cut the  $xy$  plane at various values of  $Z$ . These sections are illustrated in Fig. 3, and taken together they indicate that the trajectory of the Bloch vector is confined to a hemispheroidal shell. Further, by considering the progression of Poincaré sections it is clear that the hemispheroidal shell has scalloped edges, obviously indicating that different regions of the rotating frame's  $xy$  plane are associated with different excursions of the atomic population inversion. Studies of very many Poincaré sections for different values of  $\Omega$  show that as the dynamics change from adiabatic to nonadiabatic, the upper (positive  $Z$ ) portion of the adiabatic spheroidal shell collapses in on the lower portion, creating in the process a hemispheroidal shell. It is during this process of collapse that the highly structured transitional geometry appears in the Poincaré sections, as illustrated in Fig. 2(b). The

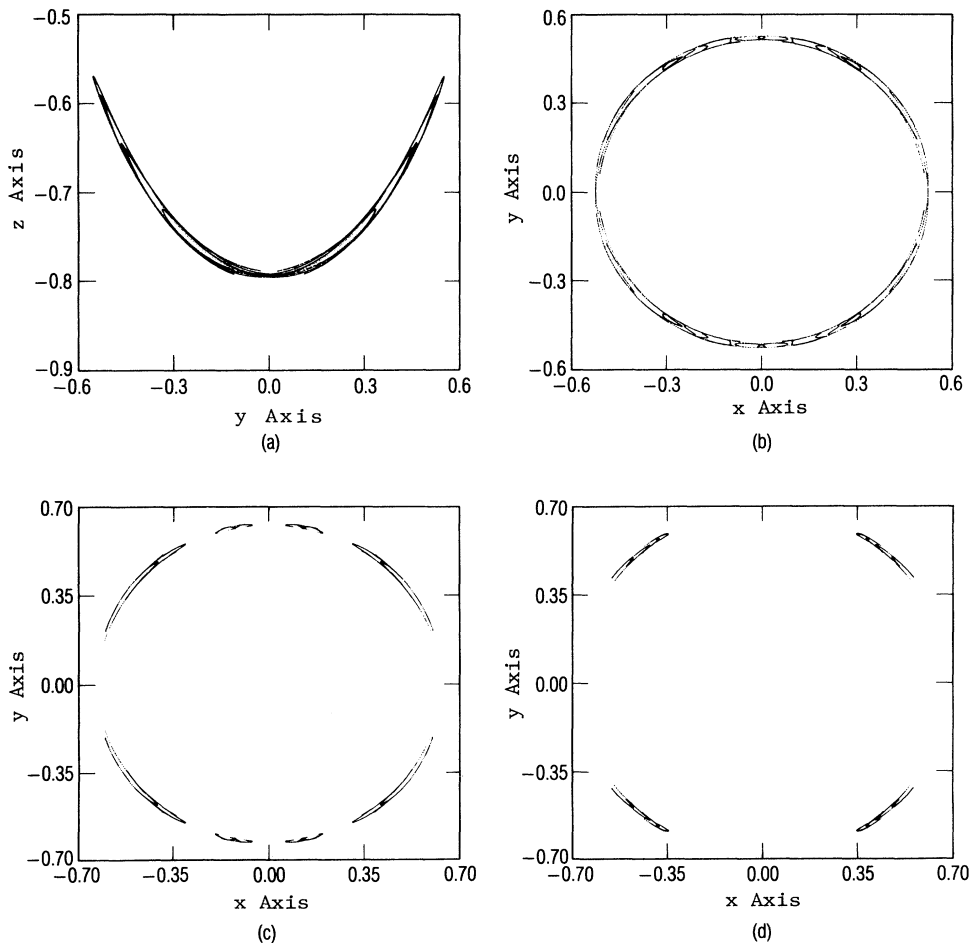


FIG. 3. Poincaré sections of Bloch vector's motion in the nonadiabatic regime ( $\Omega = 400$ ) showing scalloped edges. (a) Poincaré section through the  $yz$  plane at  $X=0.0$ . Poincaré sections through the  $xy$  planes at (b)  $Z = -0.6$ , (c)  $Z = -0.48$ , and (d)  $Z = -0.4$ .

transition region between the two limiting geometries illustrated by Figs. 2(a) and 2(c) is relatively narrow, corresponding to roughly a 10% change in  $\Omega$ .

These observations concerning the groups of double-Poincaré sections are quite revealing. Specifically, they indicate that even though the temporal evolution of the atomic dynamics is difficult to categorize (consider Fig. 1), the attractor geometry typically falls into one of two limiting categories. There is a geometrical category for adiabatic dynamics, and a geometrical category for nonadiabatic dynamics. (We will not consider the possibility of a third category associated with the transition from nonadiabatic to adiabatic dynamics.) Thus attractor geometry is apparently controlled to a large extent by the single parameter  $\eta$ , and there is a critical value of  $\eta$  about which the attractor geometry changes fairly abruptly. In the following section we will look in a more quantitative fashion at how the attractor geometry depends on  $\eta$ .

### B. Correlation dimension $\nu$

The Grassberger-Procaccia correlation integral  $C(r)$  is basically defined as the probability of finding two points on the attractor within a distance  $r$  of each other, where  $r$  is called the “scaling length.” In many, though not all, cases it is found that  $C(r)$  displays a power-law dependence on  $r$  with exponent  $\nu$ <sup>15</sup>:

$$C(r) \sim r^\nu. \quad (4)$$

The usefulness of  $\nu$  as a measure of attractor geometry is that it is a lower bound on the Hausdorff dimension  $D$  of the attractor, which in turn can be considered as the “scaling” dimension of the geometrical entity.<sup>21,22</sup> In the case of a uniformly covered attractor  $\nu$  is equal to the Hausdorff dimension.

An example of the dependence of the correlation integral on scaling length is shown in Fig. 4(a), and two different correlation dimensions are apparent. For small scaling lengths the attractor geometry yields  $\nu_s \sim 3$  (we will have more to say on the exact value of this exponent later), while for larger scaling lengths the attractor geometry is described by  $\nu_a = 1$ . Though the figure corresponds to the specific case of  $\eta = 10$  ( $\Omega = 17772$ ), these two distinct correlation dimensions were obtained at all values of  $\eta$  (i.e., Rabi frequency) investigated:  $10^{-3} < \eta < 20$ . Therefore, we picture the attractor as a geometrical entity which looks macroscopically like a curve, but on closer examination is actually a hypersurface. Further, this overall picture of the attractor cannot change too radically as a function of adiabaticity, since the two distinct correlation dimensions were always obtained.

Note that the scaling length  $r_a$ , illustrated in Fig. 4(a), indicates the maximum size of the attractor, and that  $r_s$  is related to the maximum extent of the attractor’s hypersurface portion. The ratio  $r_s/r_a$  is therefore a measure of the relative size of the attractor’s hypersurface portion, and this ratio is plotted in Fig. 4(b) as a function of the adiabaticity parameter  $\eta$ . As the figure clearly shows, there is a large increase in  $r_s/r_a$  near  $\eta \sim 1$ , and that around this maximum there are resonancelike features.

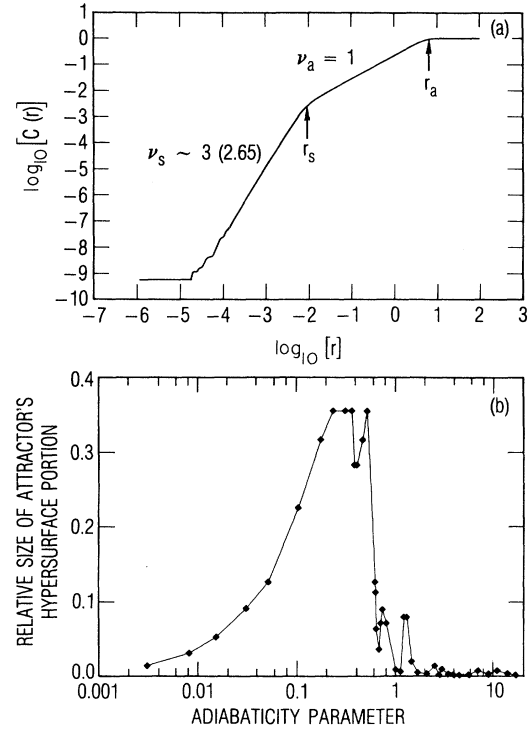


FIG. 4. (a) Logarithm of the correlation integral  $C(r)$  vs the logarithm of the scaling length  $r$  for the case of  $\Omega = 17772$ . Note the two different scaling regions with  $\nu_s \sim 3$ , and  $\nu_a = 1$ . The actual value of  $\nu_s$  obtained by a least-squares fit to the curve is shown in parentheses.  $r_s$  and  $r_a$  are related to the size of the attractor’s hypersurface portion and size of the whole attractor, respectively. (b) Variation in the relative size of the attractor’s hypersurface portion ( $r_s/r_a$ ) with adiabaticity parameter  $\eta$ .

We have found that these resonant increases in the attractor’s hypersurface portion are correlated with enhancements in the amplitude of population and coherence oscillations. Such enhancements in the transient response of a quantum system to a train of radiation-field changes have been termed Rabi resonances.<sup>16,17</sup> We are therefore led to conclude that the hypersurface portion of the attractor is intimately connected with the atomic variables of the dynamical system, rather than the field’s phase. Furthermore, since the ratio  $r_s/r_a$  is small in both the nonadiabatic and adiabatic regimes, and since the value of  $\nu_a$  is exactly the same in both regimes, the macroscopic appearance of the attractor in the two regimes cannot be very different. We therefore have an indication that the difference in nonadiabatic and adiabatic attractor geometries must be associated with the hypersurface portion of the attractor.<sup>23</sup>

If the attractor’s geometrical change is associated with the hypersurface portion of the attractor, then it should be possible to quantify the change in attractor geometry by calculating  $\nu_s$  as a function of  $\eta$ . Unfortunately, the determination of  $\nu_s$  is not always straightforward. In the nonadiabatic and transition regimes of the dynamics the

small scaling-length behavior of  $C(r)$  does not obey a simple power-law scaling relation with  $r$ . Perhaps this is not too surprising, since the groups of double-Poincaré sections in both the nonadiabatic and transition regions implied an attractor having nonuniform coverage, and for nonuniformly covered attractors one should really consider the entity as a multifractal.<sup>24</sup> In the adiabatic regime, however, the double-Poincaré section groups indicated a uniformly covered attractor, and the correlation integral  $C(r)$  does obey a simple power-law scaling relation with  $r$ . Thus we can at least examine  $\nu_s$  as a function of  $\eta$  in the adiabatic regime of dynamics.

Figure 5 shows the variation of  $\nu_s$  with  $\eta$  in the adiabatic regime of the atomic dynamics. (Error bars are statistical in nature and reflect the ability to fit a straight line through the  $\log_{10}[C(r)]$  versus  $\log_{10}(r)$  data at the 95% confidence level.) Near the transition region from nonadiabatic to adiabatic dynamics ( $\eta < 4$ ) the correlation dimension is integer:  $\nu_s = 3$ . However, for values of  $\eta$  greater than about 4, Fig. 5 indicates that the geometry of the hypersurface changes, becoming noninteger with  $\nu_s \approx 2.65$ , and under the assumption of a uniformly covered attractor this implies  $D \approx 2.65$ . [Figure 4(a) provides an example of the noninteger power-law scaling behavior of  $C(r)$  for the case of  $\eta = 10$ .] A noninteger dimension indicates that the dynamics have given rise to a *strange* attractor as described by Romeiras and Ott.<sup>25</sup> To our knowledge this is the first indication that *linear*-dynamical systems may give rise to strange attractors.

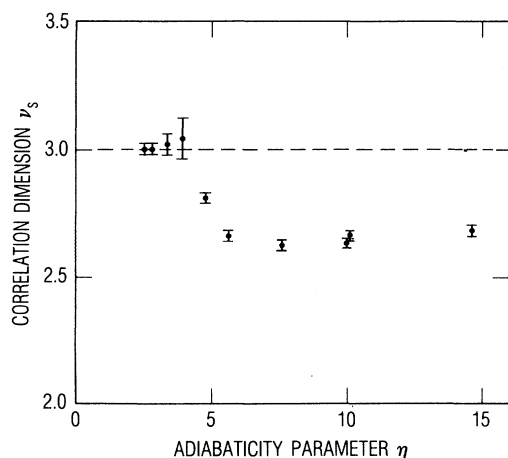


FIG. 5. Correlation dimension of hypersurface portion of attractor  $\nu_s$  vs the adiabaticity parameter  $\eta$ . These values were obtained by least-squares fits of  $\log_{10}[C(r)]$  vs  $\log_{10}(r)$ . The correlation data in all cases was obtained from at least 20000 ( $X, Y, Z, \theta$ ) coordinates spread uniformly between  $t = 12$  and 100. Close to the transition region, where the character of the dynamics changes from nonadiabatic to adiabatic,  $\nu_s = 3$ . However, in the regime where the dynamics are clearly adiabatic (i.e.,  $\eta > 4$ )  $\nu_s \approx 2.65$ . With the assumption that the attractor is uniformly covered in the adiabatic regime, this result implies that the Hausdorff dimension of the attractor is noninteger, and that the attractor is strange.

More importantly perhaps, Fig. 5 clearly indicates that the hypersurface portion of the attractor is responsible for the geometrical change in the attractor that was indicated by the groups of double-Poincaré sections, and that this geometrical change of the hypersurface is nontrivial.

Of course, with an apparently fractal attractor geometry one must wonder as to the possibility of actual chaotic dynamics for this system. We have examined the  $X, Y, Z, \theta$  trajectories, though, and find no evidence of exponential divergence upon small variations of these variables. Thus in a classical sense the system is nonchaotic. Although a strange, nonchaotic attractor for this system is surprising, it is not without precedent. Romeiras and Ott<sup>25</sup> have found that quasiperiodically forced *nonlinear* systems can give rise to strange attractors, even though the dynamics are not chaotic. Hence, chaotic dynamics are a sufficient, but not necessary condition for the existence of a strange attractor. Further, Luck, Orland, and Smilansky have found that quasiperiodic perturbations can give rise to atomic dynamics that are somewhat intermediate between quasiperiodic and chaotic. Hence one should perhaps expect nontrivial attractor geometries for quasiperiodically perturbed quantum systems.

#### IV. DISCUSSION

Our foregoing analysis has indicated that atomic dynamics in the presence of a quasiperiodic resonant field can give rise to two geometrically distinct attractors, depending upon whether the perturbation's variations are nonadiabatic or adiabatic. In order to justify these results intuitively, we note that in the standard picture of resonance phenomena the Bloch vector  $\mathbf{B}$  precesses about an axis  $\mathbf{P}$  in the rotating coordinate frame, and normally this precessional axis is aligned with the effective field  $\mathbf{E}_{\text{eff}}$ . In this rotating or "coherent," frame as Avan and Cohen-Tannoudji refer to it,<sup>26</sup>  $\theta(t)$  describes the orientation of the effective field in the  $xy$  plane, and  $\phi(t)$  describes the orientation of the Bloch vector's precessional axis with respect to the effective field. Alternatively, one can consider the Bloch vector's motion in an "instantaneous" frame,<sup>26</sup> where the  $x'$  axis is now *defined* by the effective field, and the Bloch vector's axis of precession is at an angle  $\phi(t)$  with respect to the  $x'$  axis. When the Bloch vector's components  $X, Y, Z$  or  $X', Y', Z$  are constant (or vary only little) the four-dimensional motion will be dominated by the  $0$  to  $2\pi$   $\theta$  variations, yielding an attractor dimension close to unity over most scaling lengths.

In the adiabatic regime of the atomic dynamics  $\phi(t) = 0$ , since the Bloch vector's axis of precession closely follows the motion of the effective field. Consequently, in the instantaneous frame the Bloch vector will be in near steady state with  $X', Y',$  and  $Z$  taking on small nearly constant values. Because  $X', Y',$  and  $Z$  are all typically small, we expect the attractor to be dominated by its  $\theta$  variations, and to have a dimension  $D = 1$  over significant scaling lengths. This explains the relatively small values of  $r_s/r_a$  in the adiabatic regime. However, as a result of the  $\theta$  changes which induce population and

coherence oscillations,<sup>16</sup> the Bloch vector actually oscillates slightly. Thus,  $X'$ ,  $Y'$ , and  $Z$  are not quite constant, but vary somewhat about their mean values. The Bloch vector will therefore pass through the  $x'y'$  plane in a small region of spatial extent  $\Delta\xi$ .

As viewed from the coherent frame, the Bloch vector's axis of precession will rotate in a complicated fashion about the  $z$  axis. Since  $\theta(t)$  is close to being  $\delta$  correlated when the sine and square-wave frequencies are incommensurate, and since  $\phi(t)=0$ , the various orientations of the Bloch vector's axis of precession will also be nearly  $\delta$  correlated. These erratic orientations of the precessional axis, coupled with the Bloch vector's oscillations, will thus yield a Bloch-vector trajectory in the coherent frame that appears to "weave" a geometrical entity, the "threads" of which are separated from one another in an erratic fashion. Hence the group of double-Poincaré sections in the coherent frame would have the appearance of "randomly" distributed points in an annulus of thickness  $\sim \Delta\xi$ . Furthermore, we could account for the fractal nature of the attractor in the adiabatic regime by imagining the threads of Bloch-vector trajectories to weave a fractal entity.<sup>27</sup>

In the nonadiabatic regime the phase variations of the field are rapid, so that the average field seen by the atom is small, resulting in relatively small variations of  $X$ ,  $Y$ , and  $Z$ . Therefore, we again have a situation where the attractor is dominated by  $\theta(t)$ , so that over most scales  $D$  is unity. Furthermore, in the nonadiabatic regime  $\phi$  no longer vanishes. Consequently, we ascribe the twisted Bloch-vector trajectory in the coherent frame to the combined temporal behavior of  $\phi(t)$  and  $\theta(t)$ .

## V. SUMMARY

We have shown that a careful study of attractor geometry can be quite useful for elucidating the dynamics

of quantum systems interacting with rapidly fluctuating electromagnetic fields. In the specific case of a field whose phase varies quasiperiodically, we have found that even though the atomic dynamics appear quite complicated, they nonetheless give rise to only two limiting attractor geometries. Though in both cases the attractor is relatively simple, consisting of a hypersurface portion and a curvilinear portion, our results indicate that the geometrical characteristics of the attractor's hypersurface portion depend on the perturbation's degree of adiabaticity. Furthermore, the results suggest that in the adiabatic regime the hypersurface portion becomes fractal, so that the atomic dynamics exist on a strange attractor. To observe this fractal character, experiments would have to be performed on systems with  $\Omega \gg \gamma$  and  $\eta > 4$ . In this regard a good test system would be the ground-state hyperfine transition of  $^{87}\text{Rb}$ : (i) the transition frequency is in the microwave regime (6.8 GHz) so that fields are highly monochromatic; (ii) the relaxation associated with this transition is on the order of  $10^2$  Hz, so that easily obtained Rabi frequencies in the tens of kilohertz regime should be adequate;<sup>28</sup> and (iii) the field couples only two discrete quantum states. Experiments on this system are in progress in our laboratory. We believe that with the measures now available for quantifying attractor geometries from experimental data, the study of attractors can yield new insights into the dynamical behavior of quantum systems in the presence of complicated time-varying perturbations.

## ACKNOWLEDGMENTS

We wish to thank Dr. J. Gelbwachs for stimulating our interest in this problem, and Dr. B. Jaduszliwer for a critical reading of the manuscript. This work was sponsored by the Aerospace Corporation Research program.

<sup>1</sup>A. Z. Genack and R. O. Rickman, *Appl. Phys. B* **28**, 276 (1982); A. Z. Genack, K. P. Leung, and A. Schenzle, *Phys. Rev. A* **28**, 308 (1983); B. Macke, J. Zemmouri, and B. Segard, *Opt. Commun.* **59**, 317 (1986).  
<sup>2</sup>P. Helisto, E. Ikonen, T. Katila, and K. Riski, *Phys. Rev. Lett.* **49**, 1209 (1982); E. K. Realo, K. K. Rebane, M. A. Khaas, and Ya. Ya. Iygi, *Pis'ma Zh. Eksp. Teor. Fiz.* **40**, 477 (1984) [*JETP Lett.* **40**, 1309 (1984)]; P. Helisto, E. Ikonen, and T. Katila, *Phys. Rev. B* **34**, 3458 (1986).  
<sup>3</sup>J. Baum, R. Tycko, and A. Pines, *Phys. Rev. A* **32**, 3435 (1985); W. S. Warren, *Science* **242**, 878 (1988), and references therein.  
<sup>4</sup>Y. S. Bai, A. G. Yodh, and T. W. Mossberg, *Phys. Rev. Lett.* **55**, 1277 (1985).  
<sup>5</sup>See, for example, H. A. Cerdeira and B. A. Huberman, *Phys. Rev. A* **36**, 1382 (1987).  
<sup>6</sup>Y. Pomeau, B. Dorizzi, and B. Grammaticos, *Phys. Rev. Lett.* **56**, 681 (1986).  
<sup>7</sup>P. W. Milonni, J. R. Ackerhalt, and M. E. Goggin, *Phys. Rev. A* **35**, 1714 (1987); in *Lasers, Molecules, and Methods: Advances in Chemical Physics, Volume LXXIII*, edited by J. O.

Hirschfelder, R. E. Wyatt, and R. D. Coalson (Wiley, New York, 1989).  
<sup>8</sup>R. Badii and P. F. Meier, *Phys. Rev. Lett.* **58**, 1045 (1987).  
<sup>9</sup>A. Muriel, *Phys. Lett. A* **128**, 367 (1988).  
<sup>10</sup>N. D. Sen Gupta, *Phys. Lett. A* **134**, 170 (1988).  
<sup>11</sup>J. M. Luck, H. Orland, and U. Smilansky, *J. Stat. Phys.* **53**, 551 (1988).  
<sup>12</sup>R. Graham, *Europhys. Lett.* **8**, 717 (1989).  
<sup>13</sup>R. Loudon, *The Quantum Theory of Light* (Clarendon, Oxford, 1983).  
<sup>14</sup>P. Berge, Y. Pomeau, and C. Vidal, *Order Within Chaos* (Wiley, New York, 1984).  
<sup>15</sup>P. Grassberger and I. Procaccia, *Physica* **9D**, 189 (1983); N. B. Abraham, A. M. Albano, B. Das, G. DeGuzman, S. Yong, R. S. Gioggia, G. P. Puccioni, and J. R. Tredicce, *Phys. Lett. A* **114**, 217 (1986); D. Ruelle, *Proc. R. Soc. London Ser. A* **427**, 241 (1990).  
<sup>16</sup>J. C. Camparo and R. P. Frueholz, *Phys. Rev. A* **38**, 6143 (1988).  
<sup>17</sup>U. Capper and H. Mueller, *Ann. Phys. (Leipzig)* **42**, 250

- (1985).
- <sup>18</sup>G. Birkhoff and G. -C Rota, *Ordinary Differential Equations* (Xerox College, Lexington, MA, 1969), p. 165.
- <sup>19</sup>J. C. Camparo and R. P. Frueholz, *Phys. Rev. A* **30**, 803 (1984).
- <sup>20</sup>W. H. Press, B. P. Flannery, S. A. Teukolsky, and W. T. Vetterling, *Numerical Recipes* (Cambridge University Press, Cambridge, 1986) Chap. 15.
- <sup>21</sup>B. B. Mandelbrot, *The Fractal Geometry of Nature* (Freeman, San Francisco, 1983).
- <sup>22</sup>G. Mayer-Kress, *Phys. Bull.* **39**, 357 (1988).
- <sup>23</sup>Since the maximum extent of the hypersurface portion occurs in the transition region between nonadiabatic and adiabatic dynamics, it is interesting to speculate on the necessity of the density-matrix elements to achieve some maximal dispersion in-phase space in order for the attractor to make its transition from a nonadiabatic geometry to an adiabatic geometry.
- <sup>24</sup>T. C. Halsey, M. H. Jensen, L. P. Kadanoff, I. Procaccia, and B. I. Shraiman, *Phys. Rev. A* **33**, 1141 (1986); J. A. Glazier and A. Libchaber, *IEEE Trans. Cir. Sys.* **35**, 790 (1988); see also, H. Gould and J. Tobochnik, *Comput. Phys.* **4** (2), 202 (1990).
- <sup>25</sup>F. J. Romeiras and E. Ott, *Phys. Rev. A* **35**, 4404 (1987).
- <sup>26</sup>P. Avan and C. Cohen-Tannoudji, *J. Phys. B* **10**, 155 (1977). Note that in this work  $x'-y'$  corresponds to the coherent frame and  $x''-y''$  corresponds to the instantaneous frame.
- <sup>27</sup>To add quantitative evidence to this heuristic discussion, we performed some preliminary calculations examining correlation exponents for the Bloch-vector trajectory's geometry in the rotating frame. For the case of  $\eta=17$  we found that  $\log_{10}[C(r)]$  was linear in  $\log_{10}(r)$  to very small scaling lengths, and that  $\nu=1.84\pm 0.01$ . Assuming that the entity is uniformly covered, this implies that the Bloch vector traces out a fractal geometrical entity in the adiabatic regime.
- <sup>28</sup>J. C. Camparo, R. P. Frueholz, and H. G. Robinson, *Phys. Rev. A* **40**, 2351 (1989).